Cite this article
Sakellariadis L, Agalianos A, Drosos V and Anastasopoulos I
Modelling effects in centrifuge pile testing: implications on rocking response of pile groups.
International Journal of Physical Modelling in Geotechnics,
https://doi.org/10.1680/jphmg.26.00022

Research Article
Paper 2600022
Received 15/01/2026; Accepted 09/05/2026

International Journal of Physical Modelling in Geotechnics

Modelling effects in centrifuge pile testing: implications on rocking response of pile groups

Lampros Sakellariadis
Institute for Geotechnical Engineering, ETH Zurich, Zurich, Switzerland; presently GR8 GEO Engineering Consultants, Athens Greece (corresponding author: lsakellariadis@gr8-geo.com)

Athanasios Agalianos
Institute for Geotechnical Engineering, ETH Zurich, Zurich, Switzerland

Vasileios Drosos
GR8 GEO Engineering Consultants, Athens, Greece

Ioannis Anastasopoulos
Institute for Geotechnical Engineering, ETH Zurich, Zurich, Switzerland

This paper presents a series of centrifuge tests on the axial response of a single, 15 m long, 1 m dia., non-displacement pile on dense dry sand. To quantify scale effects, the pile is subjected to axial compression and tension at two different scales (1:50 and 1:100). To explore installation effects, the model piles are installed by two different methods: (a) pre-installed buried (adopting two different pluviation techniques) and (b) monotonically jacked at 1g. In addition, two distinct interface conditions are investigated using either epoxy-sand coating on aluminium piles or micro-concrete, both targeting rough conditions, matching the prototype bored reinforced concrete piles. Important aspects are further evaluated through numerical simulations, employing both conventional small-deformation three-dimensional finite element analyses and the coupled Eulerian–Lagrangian scheme for large deformations. In addition, conventional constant normal load interface tests supplement the study. The key outcomes of the study are further extrapolated to the rocking response of pile groups subjected to combined loading. Employing simple analytical models, the implications of centrifuge modelling on the rocking stiffness and moment capacity of pile groups are documented and quantified. Guidelines are provided for careful transition from model to prototype scale, accounting for the inherent limitations of centrifuge modelling on the studied problem.

Keywords: centrifuge modelling/piles & piling/scale effects

Notation

Experimental and numerical study

D_{50}	mean grain size
D_r	relative density
D	pile diameter
p'	mean effective stress
q	deviatoric stress
u	shear displacement (interface test)
V	vertical force (model or prototype)
w	vertical displacement
γ_{oct}	octahedral plastic shear strain magnitude
δ	interface friction angle
ε_s	shear strain
ε_v	volumetric strain
μ	friction coefficient
ϕ	friction angle
ψ	dilation angle

Analytical model

a	hardening parameter
K_R	pile group global rocking stiffness
$K_{R,\text{axial}}$	pile group rocking stiffness stemming from the axial stiffness of the piles
$K_{\text{t,group}}$	tangential rocking stiffness matrix of the pile group
$K_{v,t}$	tangential axial stiffness/single pile
s	pile spacing
$K_{R,b}$	pile group rocking stiffness stemming from the bending stiffness of the piles
M_{ult}	moment capacity pile group (only from axial loading of the piles)
V_o	static vertical loading
V_{po}	pullout capacity single pile
V_y	ultimate axial resistance (single pile) in the absence of hardening
X_G	transformation matrix accounting for the position of each pile
w_y	reference settlement controlling the initial axial stiffness (single pile)
θ	pile group rotation

1. Introduction

The response of pile groups subjected to combined axial and lateral loading, and overturning moment is critical for a wide range of engineering applications. One such example is overpass bridges founded on pile groups, where due to the slenderness of the

superstructure the moment capacity of the foundation is commonly the critical design factor. The moment resistance of pile foundations stems from two distinct mechanisms: (i) moment mobilised through axial loading of the piles due to their distance to the centreline of the group and (ii) moment mobilised at each pile-head due to pile bending. This paper focuses on the first mechanism (i.e. axial loading), which is often the dominant (e.g. Sakellariadis and Anastasopoulos, 2024a).

Most of the available design methodologies are still lacking experimental support, primarily due to the difficulty of performing large-scale field tests on realistic pile geometries and pile group layouts. Centrifuge modelling remains the most cost-efficient method to study experimentally such foundations. Nonetheless, it should be noted that centrifuge testing also comes with certain unavoidable limitations, primarily associated with scale effects. Guidelines on how to minimise scale effects on the tip resistance of the model piles are provided by Bolton et al. (1999) and Garnier et al. (2007). However, it is recognised that shaft resistance is prone to unavoidable scale effects (Fioravante, 2002; Garnier *et al*., 2007; Lehane et al., 2005). Furthermore, modelling choices in centrifuge testing of deep foundations are also expected to affect the experimental outcome. Recent studies on monopiles in sand demonstrate considerable installation (Fan et al., 2021) and modelling effects (Klinkvort et al., 2018; 2025).

This paper studies the axial response of single piles in compression and tension at different scales, installation methods, and pile–soil interface conditions, allowing us to identify deviations of the reduced-scale tests from the conditions of the prototype. The centrifuge study is complemented by numerical analyses, employing both conventional small-deformation finite element (FE) and large deformation coupled Eulerian–Lagrangian (CEL) schemes. In addition, constant normal load (CNL) direct shear interface tests supplement the study with respect to the pile–soil interface conditions. The observed limitations of centrifuge modelling on the studied problem are further consolidated using simple phenomenological models, expanding to the rocking stiffness and the moment capacity of pile groups.

2. Centrifuge modelling

A series of eight centrifuge tests was performed to evaluate the impact of scale effects, interface, and installation method on the axial response of a single bored pile. The prototype problem at hand refers to a single, 15 m long, 1 m dia., non-displacement pile on dense dry sand. Figure 1 illustrates the different tasks of the centrifuge campaign, while a brief overview of the tests performed is provided in Table 1. With the exception of tests SNF-A07 and SNF-A08, all of the models were created using a curtain-type air-pluviation system, calibrated to consistently achieve 85% (±5%) relative density (dense conditions). Aiming to explore the effects of the pluviation method, Tests SNF-A07 and SNF-A08 employed a hopper-type air-pluviation system, calibrated to achieve the same relative density (Alber, 2025). The achieved average relative densities are collected in Table 1, showing satisfactory consistency. Perth sand was used for the tests, which is a well-characterised and documented fine-grained sand. Based on Sakellariadis et al. (2023) and Sakellariadis and Anastasopoulos (2024b), Table 2 offers a summary of the key soil properties. The instrumentation layout is depicted in Figure 1, while details regarding the sensor type and application range are given in Table 3.

All tests were displacement-controlled at a slow rate of 0.01 mm/s to avoid undesired rate effects. Regarding the 1g-jacking installation, the selected rate was 0.1 mm/s. All processes used a stepper motor actuator (FESTO ESBF-BS63-100-5P) with a 7 kN capacity and a maximum stroke of 100 mm. The actuator was connected to the model piles by means of sliding hinges (Figure 1). This special connection allows the pile to freely settle during spin-up, avoiding the development of undesired negative skin friction. It has been successfully implemented and discussed in our previous work (Sakellariadis et al., 2023; 2026).

With respect to the model piles, two different techniques are employed. Most of the tests employed solid-section aluminium piles, scaled to either 1:50 or 1:100. In both cases, the diameter of the piles was intentionally somewhat lower than the target one, considering the thickness of the epoxy-sand coating (≈1 mm). The coating was materialised using an instant multipurpose 2-component epoxy mix (Araldite® RAPID) and the same (Perth) sand used for the soil model. The second technique, miniature reinforced concrete (RC), was employed in one test only (SNF-A08) at a 1:50 scale. The miniature RC was made of a mixture of cement and Perth sand (used as scaled aggregates), targeting C35 (cylinder) strength (verified with unconfined-compression tests). A three-dimensional (3D) printed steel reinforcement cage was employed, aiming at 1% longitudinal reinforcement and typical transverse hoop reinforcement. This technique is favourable when studying piles under lateral loading (e.g. Del Giudice et al., 2022; Knappett et al., 2011; Loli et al., 2014), as it allows a more realistic representation of the prototype RC piles. The differences in terms of axial stiffness of the structural member (aluminium against miniature RC) are expected to have negligible effects.

Given that the experiments presented in this paper were the first tests ever performed in the newly established ETH Zurich (ETHZ) beam centrifuge, a key aspect of this campaign was to ensure repeatability of all elements of the experimental procedure. Figure 2 presents the repeatability assessment for both installation techniques at 50 g. The excellent matching of the entire range of the examined response, in compression and tension, increases our confidence in the implemented experimental procedures. The same applies to the relative density of the model, as documented in Table 1. In the following sections, the results of the tests are

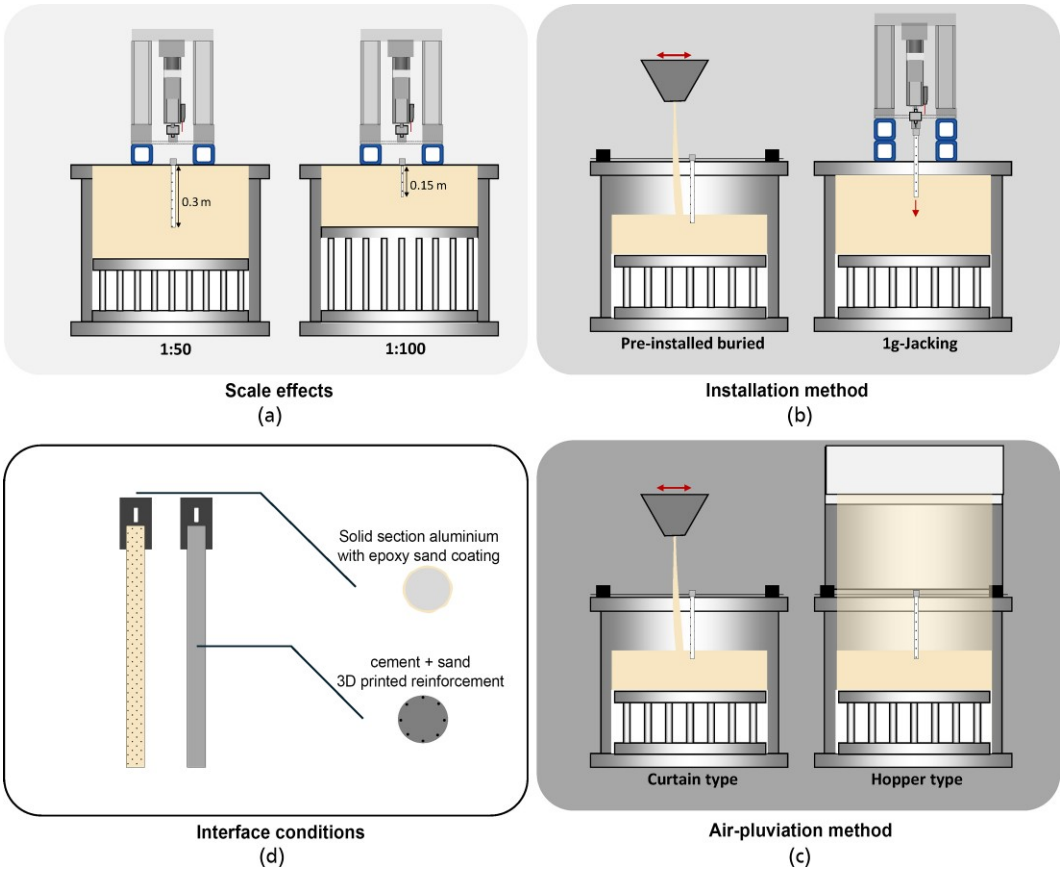

Figure 1. Overview of the experimental setup: (a) model piles scaled 1:50 or 1:100; (b) pile installation: pre-installed buried or monotonically jacked under 1g conditions; (c) different interface conditions based on the material of the model pile; and (d) employed pluviation methods

Table 1. Overview of the experimental campaign

Test ID	Scale	Installation	Pluviation	Interface	Comments	D_r: %	Date
SNF-A01	1:50	Pre-installed buried	Curtain	Solid-section aluminium	—	84	15/09/2023
SNF-A02	1:50	1g-Jacking		Epoxy-sand	—	84	19/09/2023
SNF-A03	1:50	1g-Jacking		Coating	Repeatability	85	20/09/2023
SNF-A04	1:50	Pre-installed buried			Repeatability	86	26/09/2023
SNF-A05	1:100	Pre-installed buried			—	84	29/09/2023
SNF-A06	1:100	1g-Jacking			—	85	28/09/2023
SNF-A07	1:50	Pre-installed buried	Hopper		—	93	19/06/2025
SNF-A08	1:50	1g-Jacking		Miniature RC	—	93	13/06/2025

classified and discussed separately, exploring the various aspects of physical modelling under consideration.

2.1 Scale effects

It is well-recognised that pile testing in a geotechnical centrifuge is not fully immune to scale effects. The latter can be minimised by observing the relevant guidelines with respect to the ratio of model pile diameter, D, to mean grain size, D_{50} (Bolton et al., 1999; Fioravante, 2002). Given the mean grain size of Perth sand used in all tests, $D_{50} = 0.22$ mm those recommendations are also met at 100 g ($D/D_{50} = 45$). The modelling-of-models procedure was carried out to identify and quantify the remaining scale effects: the same prototype problem was studied under two different scales: 1:50 and 1:100. The results are compared in Figure 3 for

Table 2. Soil parameters of Perth sand used in the experiments

Parameter	Value	Description
USCS	SP	Classification
D_{10}	0.14	Effective particle size: mm
D_{50}	0.22	Average particle size: mm
C_u	1.79	Uniformity coefficient
D_r	85	Relative Density
ρ_d	1720	Dry density: kg/m^3
e_{min}	0.502	Minimum void ratio
e_{max}	0.82	Maximum void ratio
ϕ'_{cv}	29.6	Critical state friction angle: °

Table 3. Devices and sensors used in the test campaign

Equipment	Type	Range
Actuator	FESTO ESBF-BS63-100-5P	Load: 7 KN/ stroke: 100 mm
Loadcell	HBK U2B	10 kN
Laser	MicroEpsilon OptoNCD	50 mm

the buried piles (compression and tension) in terms of load–deformation response in model and prototype scale. The same results are shown in Figure 4 for the piles installed by 1g-jacking. For both installation methods, the results appear affected by the g-level, particularly regarding the tensile response.

Focusing on the tensile response, the results verify a well-documented limitation of centrifuge modelling of piles: the displacement needed to fully mobilise the ultimate pullout resistance is more-or-less the same, irrespective of the g-level (Lehane and White, 2005; Lehane et al., 2005). The measured absolute displacements corresponding to full mobilisation of the pullout resistance of the model piles (both at 50 and 100 g) are similar to the expected displacement required to mobilise the shaft resistance of the prototype piles (a few millimeters). Given the rough interface conditions, the shaft resistance is mobilised through shearing within the soil instead of interface sliding. The shear deformation is concentrated within a narrow zone around the perimeter of the pile, eventually forming a shear band. Since the thickness of the shear band is primarily a function of the grain size (Cesaro et al., 2025; Loukidis and Salgado, 2008), the absolute displacement required to fully mobilise the shaft resistance does not change with the g-level. This constitutes an important limitation when presenting the experimental results on a prototype scale. Applying typical scaling laws (Garnier et al., 2007), the axial stiffness of the pile under tension appears to be reducing with the increase of the g-level, unavoidably affecting the rocking stiffness of pile groups, as discussed in the following sections.

The pull-out resistance was expected to increase with the g-level, as the ratio between the model pile diameter, D to the mean grain size, D_{50}, reduces (Lehane et al., 2005), due to the dilation of the shear band. Our experimental results indicate that this is not the case. This might be attributed to the relatively high ratio $D/D_{50} = 45$ at 100 g. According to Fioravante (2002), when $D/D_{50} > 30 - 50$ the scale effects on the shaft capacity are small (stricter limits set by Garnier and König, 1998). It could also be related to the preceding compressive loading phase (up until conventionally-defined capacity is reached), where significant shearing occurs, causing dilation effects to diminish. To that end, the general validity of this experimentally observed trend cannot be confirmed at this stage.

With respect to compressive pile response, the results appear to be less sensitive to the g-level, both in terms of initial stiffness and hardening at larger displacements. Compared to the pull-out response, the qualitative difference in initial stiffness is mainly

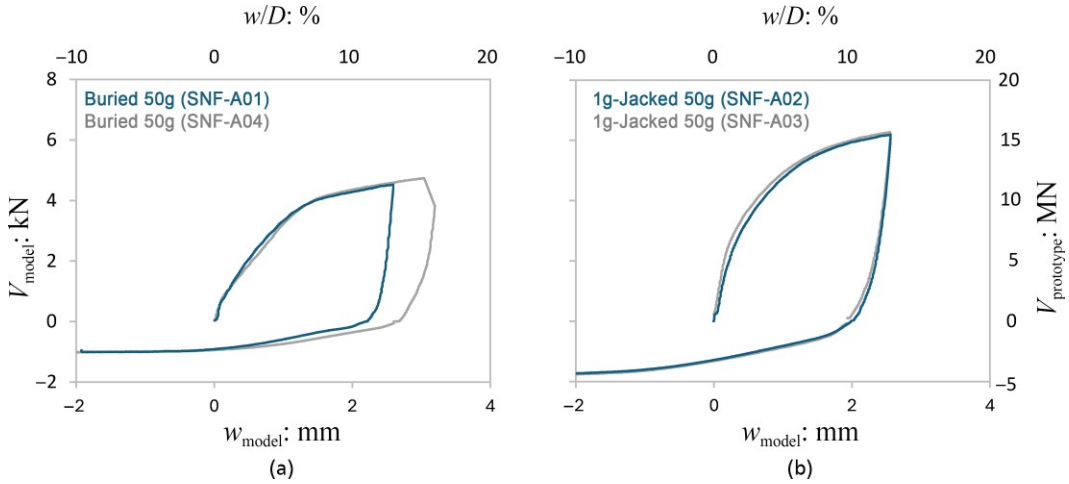

Figure 2. Repeatability assessment, load–displacement curves under compression and tension at 50 g for: (a) pre-installed buried and (b) 1 g-jacked piles. The results are presented in model and prototype scale

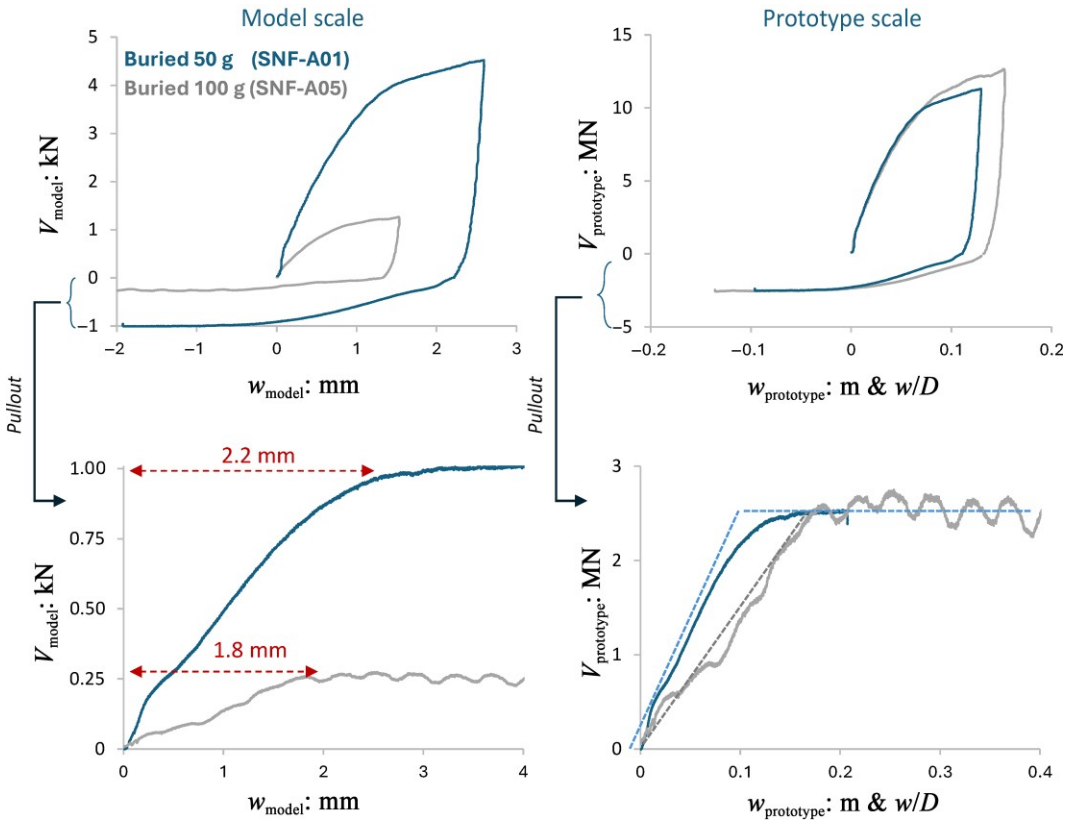

Figure 3. Quantification of scale effects for pre-installed buried piles tested at 50 and 100 g: load–deformation response in model (left) and prototype (right) scale for compression and pull-out

attributed to the considerable resistance stemming also from the tip (typical for piles in dense sand), in addition to the shaft resistance. Although the piles were not instrumented, and it is therefore not possible to distinguish precisely between shaft and tip resistance, the mobilised tensile resistance up to the pull-out capacity provides a relatively reliable means to estimate the shaft resistance also for the compression case. Following such an approximate procedure to isolate the contribution of the tip, we observe that the latter is considerable for the entire range of compression. In the small-deformation range, this trend contradicts established knowledge on the behaviour of piles in the field, where the shaft resistance governs almost exclusively this range of response. The lack of stiffness contrast between the two mechanisms (tip and shaft) in the model piles is a key difference from the pile behaviour in the field. Isolating the tip resistance for the two scales examined, it may be deduced that it is not sensitive to the g-level, in accord with the recommendations of Bolton et al. (1999) for $D/D_{50} > 20$.

2.2 Installation method

The same comparisons are performed, focusing on the effect of the installation method in function of g-level. As shown in Figure 5, consistently for both g-levels the 1g-jacked pile mobilises a larger resistance compared to the buried pile. As revealed by the mobilised pull-out capacity, a significant part of the difference stems from the shaft resistance. At the same time, the additional difference related to the tip resistance indicates that the latter is also sensitive to the installation method. A plausible explanation of the observed difference in response is that: (a) the buried pile is prone to shadowing effects, due to the curtain-type pluviation system employed herein and (b) the 1g-jacking installation is expected to cause certain density changes and extensive shearing in the pile vicinity. An additional evaluation of the results is performed later on, assisted by numerical modelling.

2.3 Interface roughness

As previously discussed, in most of the experiments, the piles were made out of an aluminium solid-section with an epoxy-sand coating, targeting rough interface conditions, which are considered representative of uncased, cast-in-place bored piles. However, this modelling technique has certain limitations when it comes to the response of model piles subjected to combined (axial, lateral, and bending) loading. Lately, the state-of-the-art is miniature RC piles. Since the latter are prefabricated using a 3D printed casing as formwork, the interface conditions might reflect relatively smooth

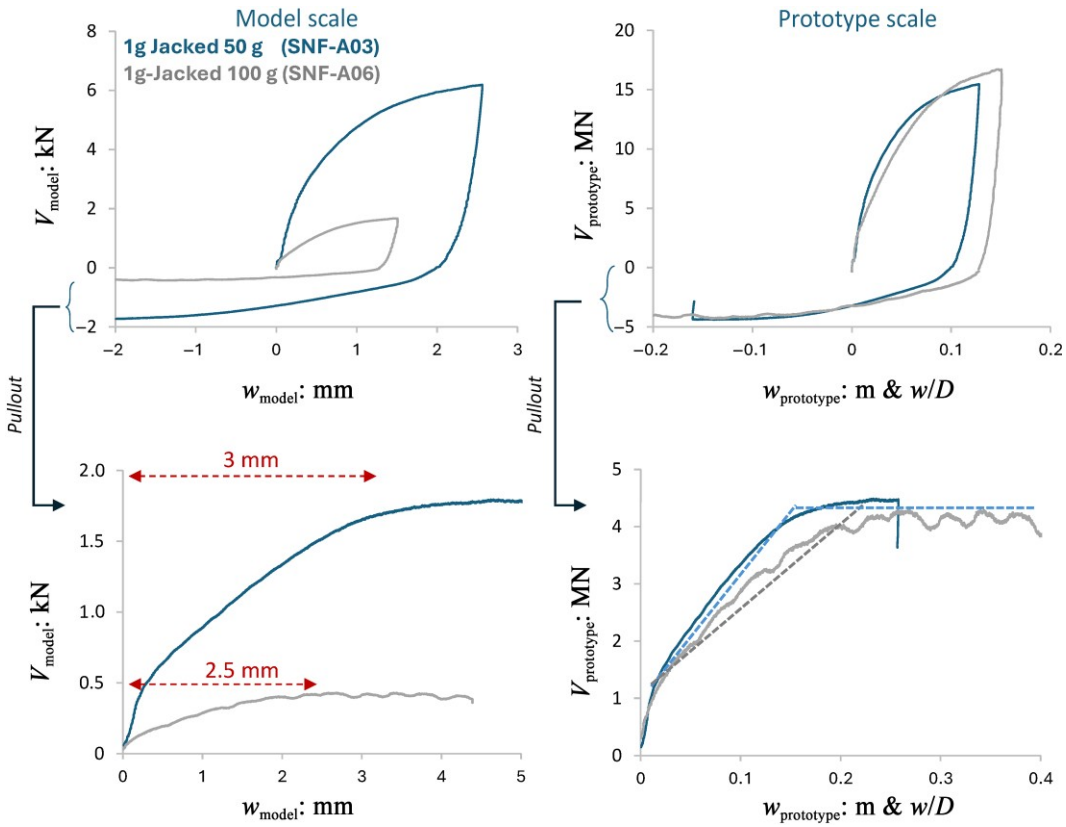

Figure 4. Quantification of scale effects for 1g-jacked piles tested at 50 and 100 g: load–deformation response in model (left) and prototype (right) scale for compression and pull-out

concrete–sand conditions. Such a pile was constructed and tested to quantify the difference between the two techniques. The results are compared in Figure 6(a) in terms of load–displacement response in model and prototype scale. The RC piles exhibit somewhat larger resistance, but this is mainly attributed to the denser state of soil in this specific test (Table 1). Overall, the two modelling approaches appear very similar in terms of mobilised shaft resistance, both achieving rough conditions. This conclusion will be evaluated further by means of CNL interface tests.

2.4 Pluviation method

All experiments presented in this work would ideally target wished-in-place (WiP) conditions. However, the results presented in Figure 5 indicate non-negligible pile-installation effects. As previously hinted, both methods unavoidably cause certain disturbance, either due to soil density change and extensive shearing in the case of the 1g-jacked piles, or due to (aerodynamic) shadowing effects during pluviation resulting in a zone of looser soil around the buried pile. To isolate the potential role of shadowing effects, the same experiment was conducted employing a different pluviation technique. Instead of the curtain-type pluviation system, a stationary hopper system was employed. Developed by Alber (2025), the system was calibrated to achieve the same target relative density. In contrast to the moving curtain-type system, the stationary system is less prone to shadowing effects and is therefore used as a benchmark for their quantification.

The two pluviation methods are compared in Figure 6(b) in terms of load–displacement response, in model and prototype scale. The response of the hopper-pluviated piles lies between the curtain-pluviated and the 1g-Jacked ones. Initially, in the small-deformation range, the response seems to be insensitive to the pluviation method. But the response changes markedly at larger deformations, especially when approaching the conventional bearing capacity limits, with the response of the hopper-pluviated pile approaching that of the 1g-jacked pile. This difference can be attributed to the shadowing effects, which are avoided to a large extent even with the stationary hopper-type pluviation system. A spot pouring hoper (e.g. Madabhushi et al., 2006) with careful local application may also be successful in reducing such undesired shadowing effects. Similar suggestions are provided for monopiles in Klinkvort et al. (2018). The 1g-jacking installation method will be further evaluated in the following section numerically.

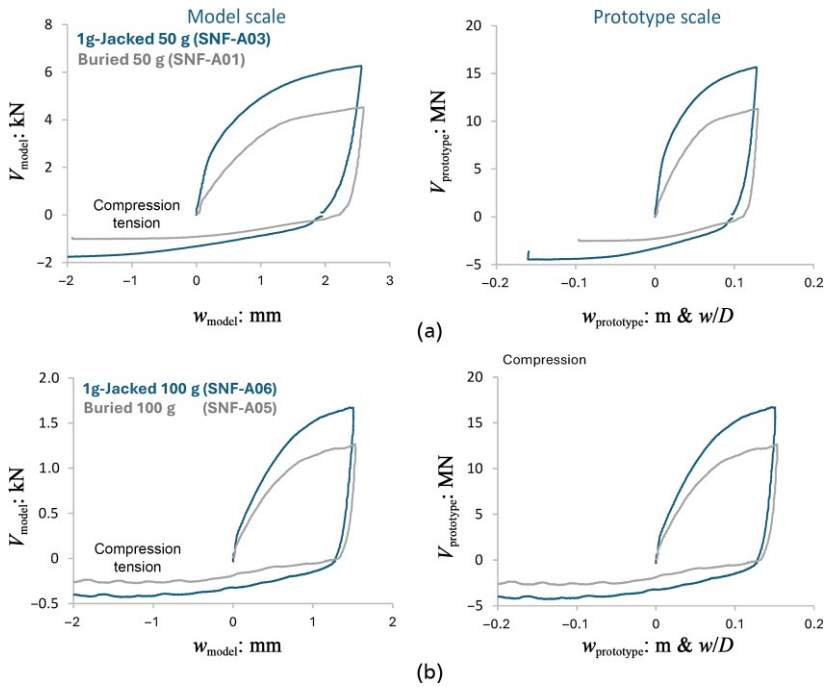

Figure 5. Quantification of installation effects. Comparison of 1g-jacked to pre-installed buried piles tested at: (a) 50 g and (b) 100 g. Load–deformation response in model (left) and prototype (right) scale for compression and pull-out

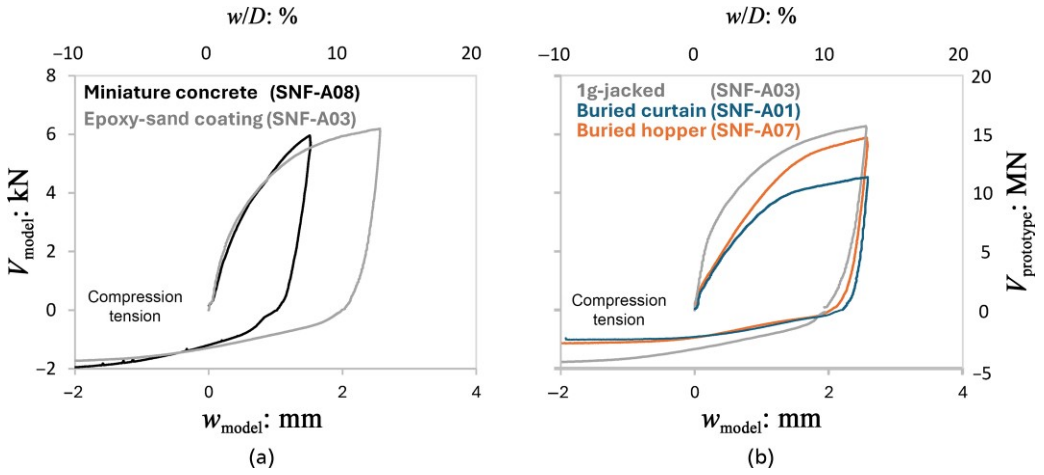

Figure 6. Influence of: (a) shaft interface, comparing solid-section aluminium piles with epoxy-sand coating (SNF-A03) to miniature RC piles (SNF-A08) tested at 50 g and (b) pluviation method, comparing a stationary hopper-type (SNF-A07) to a curtain-type (SNF-A01) pluviation system for pre-installed buried piles, compared to the 1g-jacked piles (SNF-A03), all tested at 50 g

3. Further evaluation assisted by numerical analyses and CNL interface tests

The direct interpretation of the centrifuge test results showed how certain physical modelling choices affect the axial response of the model piles. In this section, a closer look at these aspects is attempted with the help of numerical simulations (utilising conventional and large deformation FE analyses) and CNL direct shear interface tests.

3.1 Numerical study

The installation method is a key parameter controlling the response of the prototype (real-scale) piles. The same applies to

the reduced-scale piles modelled in the lab. The increased capacity and stiffness of model piles installed in flight are well-recognised in the literature (e.g. Blanc and Thorel, 2016; D'Arezzo et al. 2014; Sakellariadis et al. 2023). For the studied non-displacement (bored) piles, given the complexity of replicating the construction process both in the lab and numerically, the WiP assumption is typically adopted. With respect to our centrifuge study, all tests targeted such WiP conditions either by pluviating the sand with the pile already in place, or by means of jacking at 1g. The latter unavoidably leads to an increase of lateral stresses, which are however negligible compared to the stresses that develop after spin-up (at 50 or 100 g). The WiP condition is also favourable for validating numerical models, which typically do not incorporate installation effects implicitly (although this deviates from the field conditions).

Both installation methods were employed in the centrifuge tests and as discussed in the previous section, their differences are non-negligible in terms of pile response; at least for dense sand, such as the one examined herein. Undeniably, both approaches fail to fully ensure undisturbed conditions in the vicinity of the pile, as schematically illustrated in Figure 7. In the case of buried pile installation (Figure 7(a)), while the model pile is positioned and supported at the target location, the pluviation with the curtain-type system leads to shadowing effects, creating looser zones around the pile. As previously discussed, the extent of such disturbance is also a function of the pluviation method, with the stationary hopper-type system being less prone to such shadowing effects. On the other hand, 1g-jacking (Figure 7(b)) unavoidably leads to density change of the soil around the pile, which experiences extensive shearing during its jacking, also leading to some stress locking. The increase of the confining stresses during centrifuge spin-up is expected to reduce to some extent this disturbance. However, the spin-up itself will also lead to a certain degree of disturbance, as it deviates from the ideal WiP condition, since the soil will unavoidably settle relatively to the pile. This section aims to numerically investigate the potential effects of the spin-up process and of the 1g-jacking.

3.1.1 Constitutive model calibration

As aforementioned, the soil material used in all experiments is well-characterised Perth sand (Sakellariadis et al., 2023; Sakellariadis and Anastasopoulos, 2024b). These published data of drained isotropically-consolidated triaxial compression DIC tests (at varying consolidation pressure and relative density $D_r \approx 90\%$) were used to calibrate the MC-HS model (Agalianos et al. 2023; Agalianos and Anastasopoulos, 2021). The latter is an elastoplastic constitutive model with Mohr–Coulomb yield criterion, incorporating post-yield isotropic frictional hardening and softening. Strain hardening (and the subsequent softening) are introduced by increasing (and decreasing, respectively) the mobilised friction angle, ϕ, and dilation angle, ψ, in function of the octahedral plastic shear strain magnitude, γ_{oct}. Pre-yield behaviour is assumed elastic, described by the secant Young's modulus and Poisson's ratio, with yielding commonly assumed to take place at 50% of the maximum deviatoric stress q. The dependency of the peak friction angle and dilation angle, as well as of the elastic stiffness, on the mean effective stress p' are also accounted for. Both pressure dependency and post-yield strain hardening and softening are implemented in Abaqus through a user subroutine. More details regarding the constitutive equations of the MC-HS model can be found in Agalianos and Anastasopoulos (2021) and

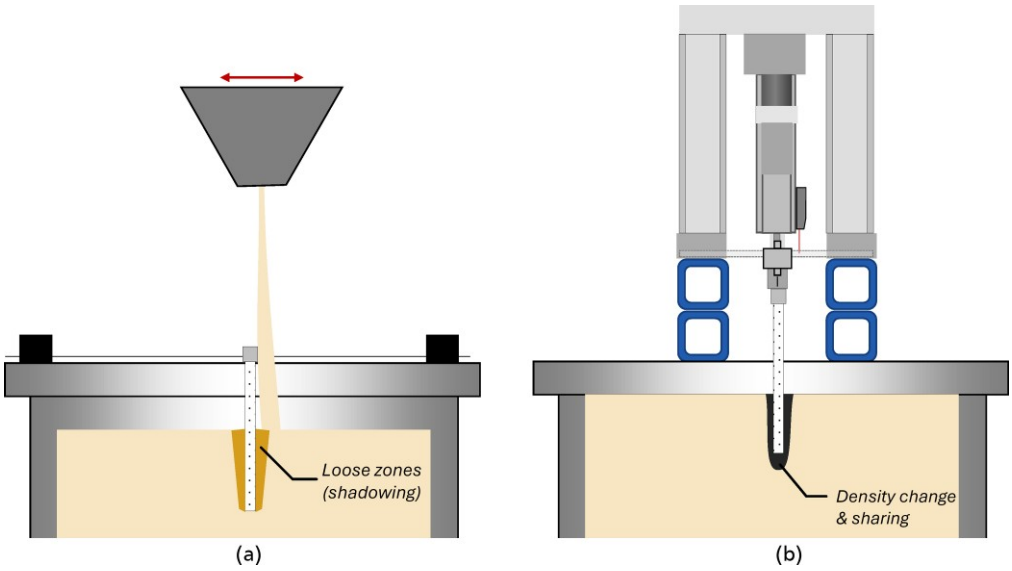

Figure 7. Expected disturbance around the pile during the preparation process: (a) pre-installed buried piles and (b) 1g-jacking installation

Agalianos et al. (2023). Figure 8 comparatively assess the behaviour of the calibrated MC-HS model against the DIC test results. Evidently, the MC-HS model successfully reproduces the deviatoric and volumetric response of the dense Perth sand used in the experiments.

3.1.2 Conventional (small deformation) FE against large deformation (CEL) analysis

This section presents the results of the numerical analyses, employing two different methods. They both correspond to model scale, focusing on centrifuge tests conducted at 50 g. First, a cost-efficient axisymmetric FE model was utilised to model the experiment, as shown in Figure 9(a). The soil and the pile are modelled with 4-node axisymmetric elements. The latter is modelled as elastic, with the material properties of aluminium. The pile surface is tied to the surrounding soil assuming full bonding (rough interface). The thickness of the first soil element near the pile is selected equal to 2 mm to match the expected shear band thickness (SBT), which is about ten times D_{50}, following the recommendation of Loukidis and Salgado (2008). It is noted that the assumption regarding the SBT is crucial in reproducing the experimental results and that a wider range of SBT is found in the literature. The selected value is seen as a lower bound (e.g. the thickness obtained applying the methodology by Cesaro et al. (2025) is 30% larger), therefore the numerical prediction is also a lower bound of the expected response. This modelling approach corresponds to WiP conditions, neglecting soil disturbance in the vicinity of the pile due to 1g-jacking or curtain-type pluviation. The FE analysis is conducted in two steps. Initially, the enhanced gravity field (50 g) is applied. Then, the pile is pushed vertically until reaching the conventional bearing capacity limit. The zones of disturbance are presented in Figure 9(a) in terms of snapshots of deformed geometry with superimposed contours of equivalent plastic strain. It is noted that during the spin-up process, due to the different density and stiffness of the soil and the pile, their relative movement results in plastic strains. The response of the model pile under compressive loading up to the conventional bearing capacity limit is shown in Figure 10 in terms of load–displacement response. The numerical prediction is in very close agreement with the experimental results for the 1g-jacked pile, especially for the initial part of the response.

The second analysis employs the CEL method, which is readily available in Abaqus (2019). The methodology is well-suited to penetration problems involving large deformations (Augarde *et al.*, 2021; Qiu et al., 2011) and is currently applied extensively to offshore applications. Recent examples of validation against centrifuge and field tests of spudcan installations can be found in Drosos et al. (2025). In this case, the analysis is performed in three steps. After applying the geostatic stress field at 1g, the pile is installed by jacking at constant velocity. The maximum

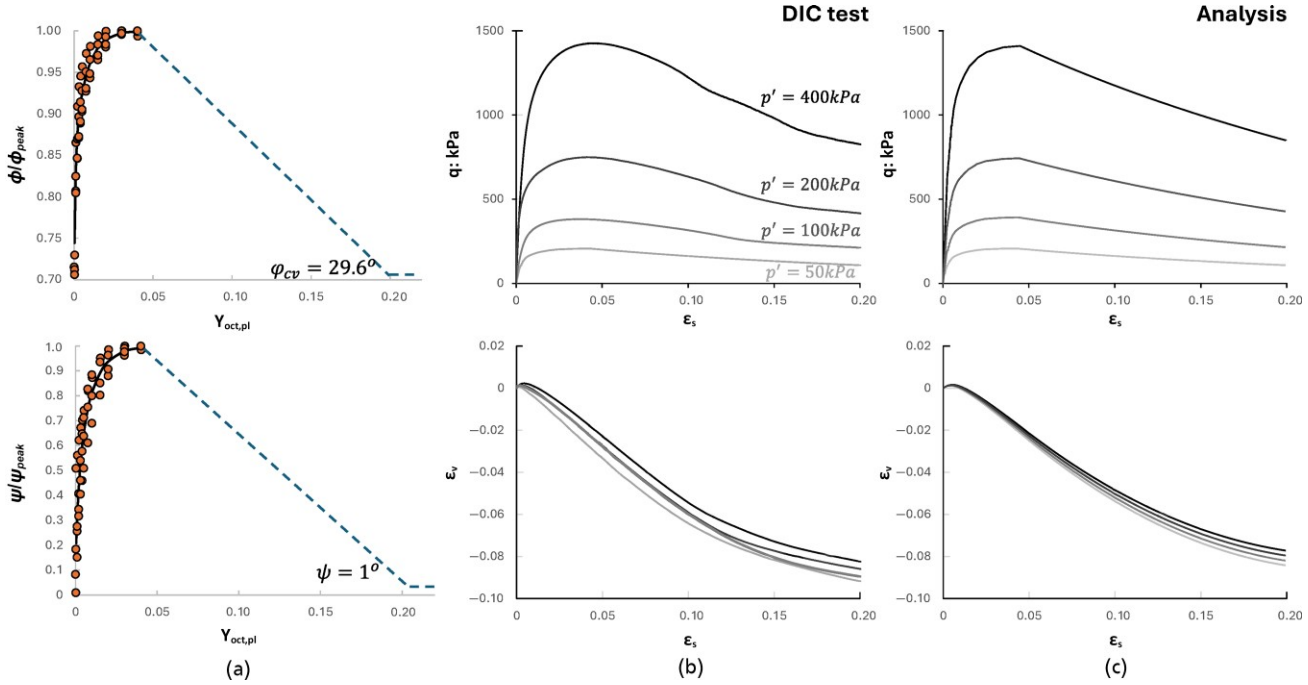

Figure 8. Comparison of the calibrated MC-HS model to triaxial compression tests conducted at ETHZ: (a) dependency of mobilised friction and dilation angle on the magnitude of plastic strain.; deviatoric and volumetric response of Perth sand derived (b) experimentally and (c) numerically after model calibration

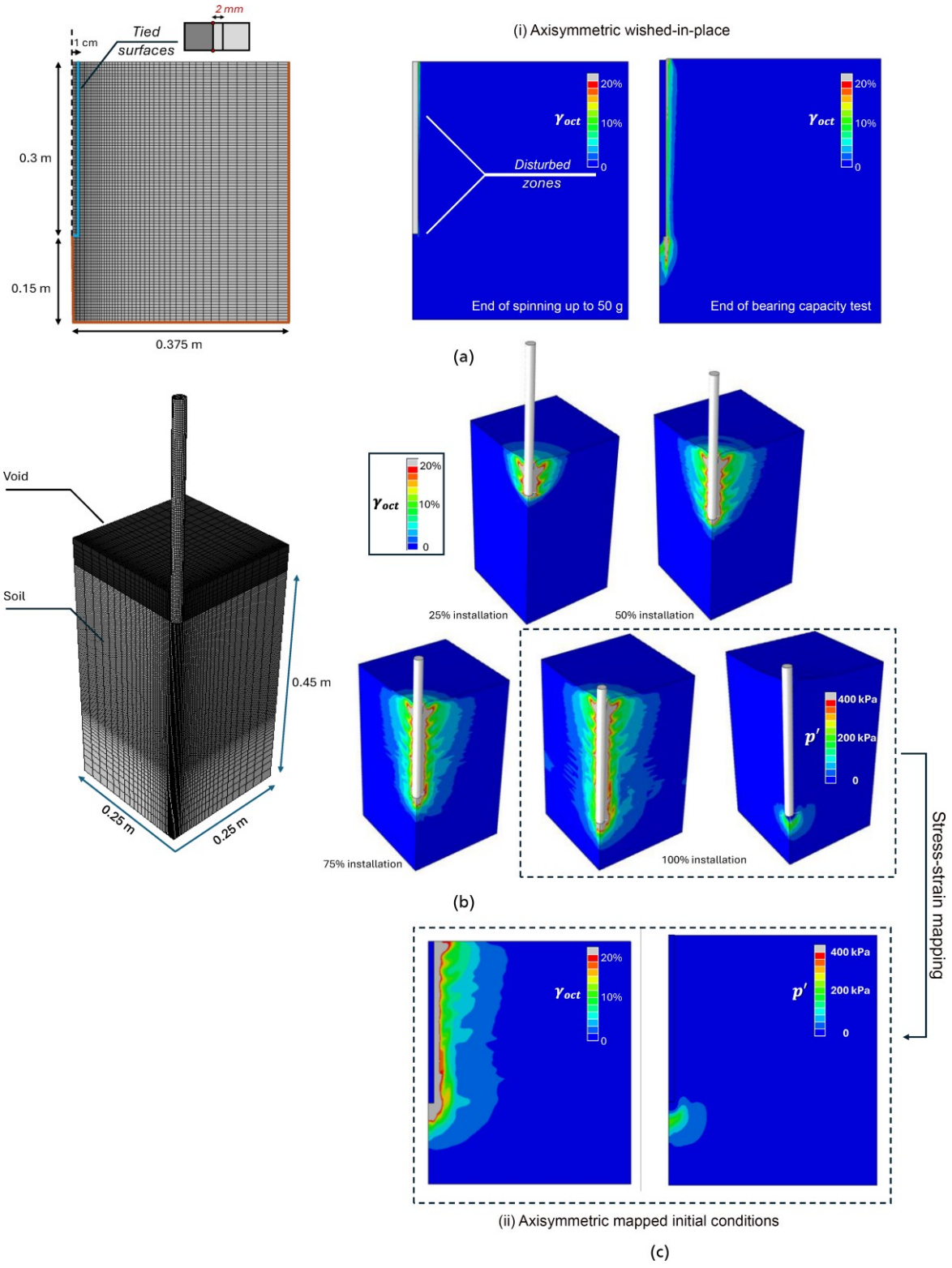

Figure 9. Geometry and key attributes of (a) the 2D axisymmetric FE analysis and (b) the 3D FE model employing the CEL scheme. The results are presented for characteristic analysis stages in terms of deformed geometry with superimposed contours of equivalent plastic strains and mean effective stress. (c) Mapping of stress–strain results of the CEL installation to initialise a 2D axisymmetric FE analysis

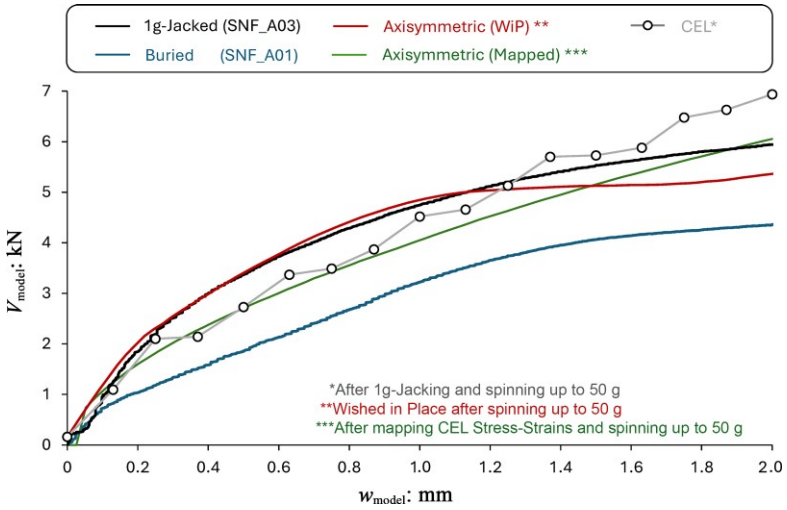

Figure 10. Comparison of centrifuge test results of 1g-jacked (SNF-A03) and pre-installed buried piles (SNF-A01) at 50 g to the numerical predictions, employing the CEL analysis, modelling the 1g-jacking installation (dotted line) or conventional axisymmetric FE analyses assuming either wished-in-place pile (red line) or initialised stress–strain field after pile installation (green line), in terms of load–displacement response

penetration resistance is found to be 1.2 kN, which is fairly close to the measured resistance (about 1 kN). Characteristic snapshots of deformed geometry with superimposed contours of plastic strains are shown in Figure 9(b). In a second step, the spin-up process is simulated by applying the enhanced gravity field. During this step, the pile moves relative to the soil due to its different density and stiffness compared to the surrounding soil. Finally, the pile is pushed downwards in a displacement-controlled manner until reaching the conventional bearing capacity limit of 0.1*D*. The mobilised resistance is presented in Figure 10, being in very close agreement with the experimental results for the 1g-jacked pile.

A third numerical analysis is performed for completeness, combining the previous two approaches. The stress and strain field at the end of 1g jacking of the CEL analysis (Figure 9(b)) is extracted and imported as an initial condition in the conventional axisymmetric FE analysis (Figure 9(c)). Following this mapping process, two steps are applied similarly to the WiP analysis, namely, application of an enhanced gravity field (50 g), and vertical compression up to the bearing capacity limits. The resulting load deformation curve is added in Figure 10 and is in close agreement with the compression curve from the CEL analysis.

Those analyses are presented without conducting any sensitivity study on potential effects of the modelling strategy, such as meshing, velocity, and other numerical parameters. To that end, the presented results should be treated more on a qualitative rather than a strictly quantitative basis. The comparison of the two analyses suggests that the effect of soil disturbance during 1g-installation is rather limited. The spin-up process also causes certain disturbance in the vicinity of the pile. The analyses are very close to the experimental results for the 1g-jacked piles, supporting the adoption of this installation method compared to the buried piles. Especially at small imposed displacement, the stiffness of the buried piles is significantly lower than both numerical analysis results. However, this conclusion requires further investigation by means of additional detailed parametric numerical and experimental studies and should not be generalised, particularly for different soil conditions (e.g. loose sand).

3.2 Constant normal load interface test

The results presented so far highlighted the importance of the shaft resistance of the model piles and of the complex mechanisms involved. To shed more light on these mechanisms, three CNL direct shear interface tests were performed and are presented herein. All tests targeted the relative density of the centrifuge tests (about 85%). Given certain limitations of the experimental setup, the maximum displacement was 7.5 mm. The first test was conducted applying monotonic loading, while the remaining two applied two-way loading. The latter were performed at the average lateral stress level acting on the pile, one for the epoxy-sand coated interface and one for the miniature RC. The monotonic loading was performed at double the stress level to quantify stress-dependency.

The results are shown in Figure 11 in terms of mobilised interface friction angle, δ, or friction coefficient, μ, in function of shear deformation, u. The CNL tests indicate limited stress dependency of the interface friction, with both surfaces yielding similar results corresponding to rough conditions. The two-way loading tests offer additional insights, with the load reversal pointing to a

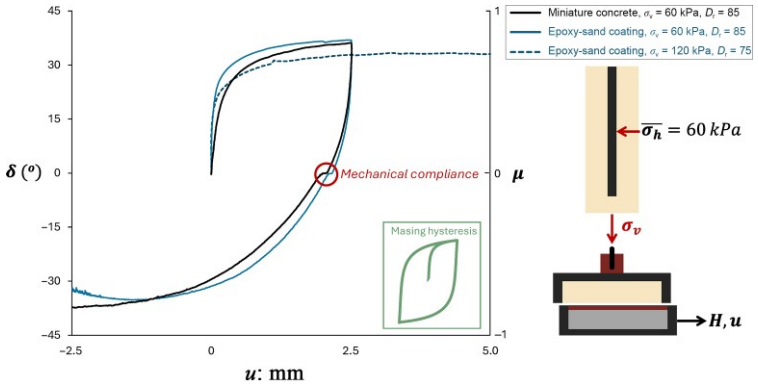

Figure 11. Constant normal load (CNL) interface tests: mobilised interface friction angle, δ, or friction coefficient, μ against shear displacement, u

hysteretic loop resembling the Masing rule. With reference to the centrifuge tests presented in Figures 2–6, it should be noted that the pull-out loading followed the compression response up to a nominal settlement of $0.1D$. Since this nominal displacement is different at each g-level, the observed tendency of slightly lower displacement needed in the 100 g tests compared to the 50 g ones can be explained by the interface tests and the observed Masing-like hysteretic response.

4. Implications on modelling of pile groups

The conclusions drawn so far refer to single piles subjected to axial loading. As previously discussed, the axial pile response dominates the response of pile groups subjected to combined moment loading and the moment resistance mobilised by way of axial pile loading is typically considerably higher than the one mobilised by pile bending (e.g. Sakellariadis and Anastasopoulos 2024a; 2024b). The two mechanisms are schematically illustrated in Figure 12. The ultimate moment capacity of a pile group and the moment sharing between the two mechanisms largely depend on the axial capacity and stiffness of each pile in the group. Simple analytical models are employed to connect the previously drawn conclusions to the response of pile groups subjected to overturning moment, which can be useful for the interpretation of centrifuge results.

4.1 Moment capacity

The calculation of the ultimate moment capacity by way of axial loading of pile groups has been covered in recent publications

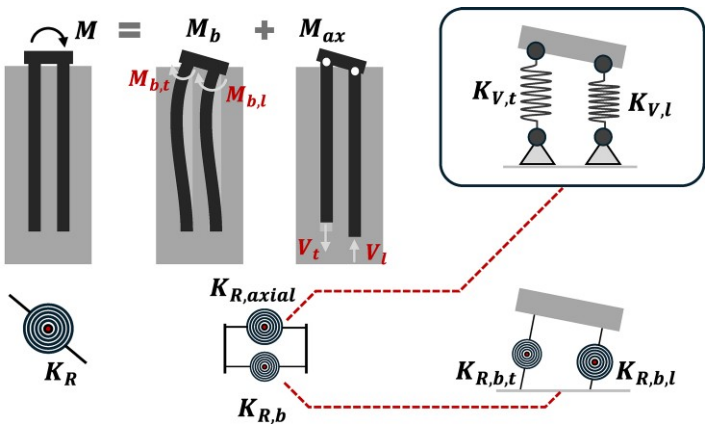

Figure 12. Illustration of the two moment resisting mechanisms for an idealised 2 × 1 pile group layout; simple spring models employed to reproduce each mechanism (Sakellariadis *et al.*, 2026). Decomposition of total rocking stiffness, K_R, in rocking stiffness stemming from the axial loading of the piles, $K_{R,\text{axial}}$, and the rocking stiffness corresponding to the bending stiffness of the piles, $K_{R,b}$. Further decomposition of $K_{R,\text{axial}}$ to vertical strings for compression and tension, and decomposition of $K_{R,b}$ to rotational springs in each pile head (function of the axial loading of each pile)

(e.g. Di Laora et al. 2019; 2025; Iovino et al. 2021; Sakellariadis and Anastasopoulos, 2024a). In our recent work (Sakellariadis and Anastasopoulos, 2024b), we emphasised the differences between plunging (clear ultimate bearing capacity) and non-plunging (performance criteria are used to define capacity conventionally) axial response on ultimate moment capacity. In the latter case, which applies for piles in dense sand (such as the ones studied herein), the ultimate moment capacity is controlled by two quantities: (i) the initial static loading of the piles and (ii) the ultimate pullout resistance of the trailing piles (given that the leading piles experience continuous hardening).

An idealised 2×1 pile group is used for illustrative purposes. Satisfying vertical load equilibrium, the ultimate moment capacity can be calculated in a straightforward manner. Assuming initial static loading $V = 2V_o$, equally shared between the piles of the group, the axial loading of the piles can only change by an equal amount dV. The leading pile is compressed further, while the trailing pile is unloaded and eventually subjected to tension. This process is limited by the pull-out resistance of the trailing pile V_{po}, and as a result $dV_{\max} = (V_{\text{po}} - V_o)$. The ultimate moment capacity for pile spacing, s, will then be:

1. $$M_{\text{ult}} = dV_{\max}\, s = (V_{\text{po}} - V_o)\, s$$

Following the results of the previous section, the pull-out resistance is sensitive to the installation method. The 1g-jacked piles exhibit 1.5 times higher resistance compared to the buried. Furthermore, a variability of roughly 15% was observed in the buried piles, depending on the employed pluviation technique (with the curtain-type pluviation being lower, due to the increased shadowing effects).

Table 4 offers a summary comparison of the pull-out resistances (prototype scale) measured in the centrifuge tests, along with the calculated ultimate moment capacity mobilised by the axial mechanism for the idealised 2×1 pile group. A static vertical load of 5 MN per pile, and a spacing $s = 3d = 3m$ are assumed. Depending on the physical modelling technique, the ultimate moment capacity ranges from 22.7 to 30.4 MNm. Following the discussion in Section 2, our study indicates that the ultimate pull-out resistance is not sensitive to the g-level. The results presented in the previous sections for 50 and 100 g show consistent maximum pullout resistance in prototype scale for each installation method. As a result, M_{ult} also appears to be g-level insensitive. This conclusion should not be generalised since there are studies indicating that when the model pile diameter approaches the SBT, a larger shaft resistance should be expected as a result of the volumetric response on the shear band (e.g. Lehane et al., 2005; Loukidis and Salgado, 2008; Sakellariadis and Anastasopoulos, 2024a). This mechanism has been discussed by Fioravante (2002), Lehane and White (2005) and more recently by Cesaro et al. (2025). A plausible explanation is that during the preceding compressive loading (at which considerable displacement is applied to the model piles), the pre-shearing along the shaft is sufficient to minimise the shear band dilation effects. As a result, during load reversal and up until the pull-out load is reached, the volumetric expansion along the shear band is rather limited. Nevertheless, more work is needed to fully explain this aspect of response.

4.2 Rocking stiffness

As previously discussed, a critical aspect is the lack of dependency between the model scale (g-level) and the displacement needed to mobilise the pull-out resistance of the model piles. This well-documented trend (Lehane and White, 2005; further confirmed by this study) has certain unavoidable effects on the rocking stiffness of pile groups tested in the centrifuge. Figure 12 presents a simple spring model to describe the macroscopic behaviour of pile groups subjected to combined loading. In a centrifuge test, the correct reproduction of the rocking stiffness of the group K_R, requires correct reproduction of both the bending stiffness of each pile ($K_{R,b,i}$) and the rocking stiffness stemming from axial pile loading ($K_{R,\text{axial}}$). While the bending stiffness of the piles (and its dependency on axial loading) can be realistically reproduced by employing miniature RC modelling (e.g. Del Giudice et al., 2022; Knappett et al. 2011; Loli et al., 2014), $K_{R,\text{axial}}$ is unavoidably sensitive to scale effects.

This section aims to quantify how $K_{R,\text{axial}}$ in the centrifuge is affected by the modelling approach, and how it compares to the

Table 4. Pull-out resistance measured in the centrifuge model tests and calculated moment capacity, mobilised by the axial mechanism for an idealised 2×1 pile group

Centrifuge test	Installation	Pluviation	Pile	g-level	V_{po}: MN	M_{ult}: MNm
SNF-A01 (04)	Pre-installed buried	Curtain	Alluminum	50	2.580	22.740
SNF-A02 (03)	1g-Jacked	Curtain	Alluminum	50	4.490	28.470
SNF-A05	Pre-installed buried	Curtain	Alluminum	100	2.750	23.250
SNF-A06	1g-Jacked	Curtain	Alluminum	100	4.290	27.870
SNF-A07	Pre-installed buried	Hopper	Alluminum	50	2.900	23.700
SNF-A08	1g-Jacked	Hopper	Miniature RC	50	5.125	30.375

prototype conditions. In this context, the simplified model of Figure 12 is employed, comprising one elastic spring in compression and one in tension for the idealised 2 × 1 pile group configuration. The springs follow the simple analytical non-linear expressions proposed by Sakellariadis et al. (2026):

$$V = V_y\left(1 - e^{-\frac{w}{w_y}}\right)(1-a) + a\,\frac{V_y}{w_y}\,w \tag{2}$$

The three model parameters, V_y (load), w_y (displacement), and a (unitless hardening parameter) are selected to fit the previously discussed experimental results at the prototype scale. The comparisons are shown in Figure 13, while the model parameters are summarised in Table 5. Regarding the pull-out response, the red dashed lines indicate the analytical fit, but this time scaling down the displacement, w_y by the corresponding g-level. This stiffer response is believed to better represent the prototype conditions.

The fitted curves are then used to estimate the entire moment–rotation response. This further depends on the initial static loading, which is assumed to be 5 MN per pile, as in the calculation of the previous section and the spacing between the piles, s. Using the analytical fit of Equation 2, the tangential axial stiffness of the piles can be expressed in a generalised way (Sakellariadis et al. 2026) as follows:

$$K_{v,t} = (1-a)K_o\left(1 - \left(\frac{V - aK_o w}{(1-a)\,V_y}\right) * \left[\frac{1}{2}\,(1 + \mathrm{sign}(\delta w V))\right]\right) + aK_o \tag{3}$$

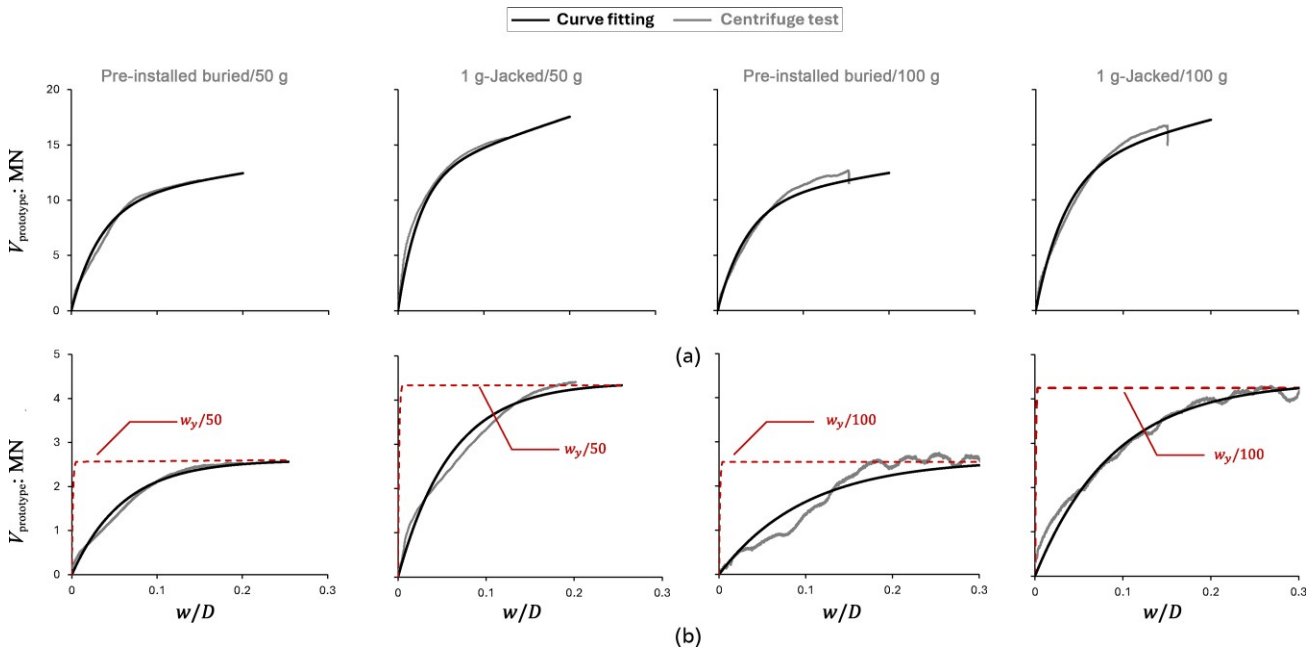

Figure 13. Curve fitting of the simplified analytical model to the experimental results at prototype scale, comparing the various installation methods at two different g-levels: (a) response in compression and (b) pull-out response

Table 5. Model parameters used for curve fitting Equation 2 to the experimental results at the prototype scale

	Compression			Tension		
Centrifuge test	V_y: kN	w_y: m	α: –	V_y: kN	w_y: m	α: –
Pre-installed, 50 g	10 500	0.035	0.04	2600	0.06	0
1g-Jacked, 50 g	13 000	0.025	0.05	4400	0.06	0
Pre-installed, 100 g	10 500	0.035	0.04	2600	0.10	0
1g-Jacked, 100 g	14 000	0.035	0.05	4400	0.09	0

assuming the different curve fitting parameters for compression and tension:

4. $$K_{\mathrm{o}} = K_{\mathrm{o,tension}} + \left(\frac{K_{\mathrm{o,comp.}}}{2} - \frac{K_{\mathrm{o,tension}}}{2}\right)(1 + \mathrm{sign}(V))$$

5. $$a = a_{\mathrm{tension}} + \left(\frac{a_{\mathrm{comp.}}}{2} - \frac{a_{\mathrm{tension}}}{2}\right)(1 + \mathrm{sign}(V))$$

6. $$V_y = V_{\mathrm{y,tension}} + \left(\frac{V_{\mathrm{y,comp.}}}{2} - \frac{V_{\mathrm{y,tension}}}{2}\right)(1 + \mathrm{sign}(V))$$

where $K_o = \frac{V_y}{w_y}$.

The incremental response of the pile group under vertical eccentric loading can then be calculated as:

7. $$\begin{bmatrix}\Delta V \\ \Delta K\end{bmatrix}_{\mathrm{group}} = K_{\mathrm{t,group}} \begin{bmatrix}\Delta w \\ \Delta \theta\end{bmatrix}_{\mathrm{group}}$$

8. $$K_{\mathrm{t,group}} = {X_G}^T K_{G,t} X_G$$

9. $$X_G = \begin{bmatrix}1 & s/2 \\ 1 & -s/2\end{bmatrix}$$

10. $$K_{G,t} = \begin{bmatrix}K_{v1,t} & 0 \\ 0 & K_{v2,t}\end{bmatrix}$$

For this calculation, a total rotation $\Delta\theta = 0.1$ rad is imposed, and the analytical model uses the four different sets of parameters given in Table 5. One more solution is obtained using the adjusted pull-out response, indicative of the 1g-jacked pile at 50 g, by reducing w_y only in tension by 50 times (red dashed line in Figure 13). Given that the displacement needed to mobilise the pull-out resistance of the model piles at 50 g is similar to that of the prototype piles (Section 2), this adjusted stiffer pull-out curve is expected to be more representative of prototype conditions. This is referred to as 'adjusted prototype'; the response in compression is not adjusted, although a stiffer response of the shaft should be expected in prototype conditions. The results are compared in Figure 14 in terms of: (a) resisting moment; (b) settlement; and (c) secant rocking stiffness as a function of rotation. The results demonstrate the sensitivity of the rocking pile group response on the modelling approach. The deviation from the expected prototype response is non-negligible, depicting the scale (g-level) dependency of the rocking mechanism, $K_{R,\mathrm{axial}}$.

This unavoidable limitation of centrifuge modelling should be kept in mind both in the initial design and in the interpretation of centrifuge model tests. Centrifuge researchers should keep in mind that scaling the bending stiffness of the structural elements properly, $K_{R,b}$ will unavoidably lead to incorrect moment sharing between the two resisting mechanisms. A potential remedy is to adjust the bending stiffness of the piles, depending on the target g-level to maintain the correct stiffness ratio that better represents the prototype conditions.

5. Conclusions

Targeting both the physical modelling community and numerical analysts, this paper has critically assessed certain modelling aspects and inherent limitations of centrifuge modelling of pile foundations. A series of centrifuge model tests was conducted, initially exploring the well-recognised scale effects of centrifuge modelling on the axial response of piles. It was shown that such effects should not be neglected when evaluating centrifuge model test results of pile foundations, especially in the case of pull-out response.

The centrifuge campaign further documented the importance of the pile installation method. The test results revealed non-negligible shadowing effects that lead to lower relative density around the pile when using a curtain-type pluviation system. The latter can be reduced by employing a stationary hopper-type pluviation system. Pile installation by 1g-jacking was shown to lead to an increased axial resistance, mainly due to the soil being displaced by the pile. The effect of the increase in lateral stresses remains limited, as they are negligible compared to the confining stresses after spin-up. These conclusions regarding the installation method were further confirmed by numerical modelling. Our combined experimental-numerical study may assist physical modellers in making informed decisions on the selection of the installation method. Combining centrifuge model tests and CNL interface tests, two pile–soil interfaces were explored, both corresponding to rough interface conditions, showing negligible deviations.

The significance of the pile installation method and scale effects was further explored with respect to the rocking response of pile groups. The latter was evaluated by analysing an idealised 2×1 pile group, adopting a simplified analytical model. It was shown that the rocking stiffness and the moment capacity of a pile group are not immune to scale effects, mainly related to the displacement

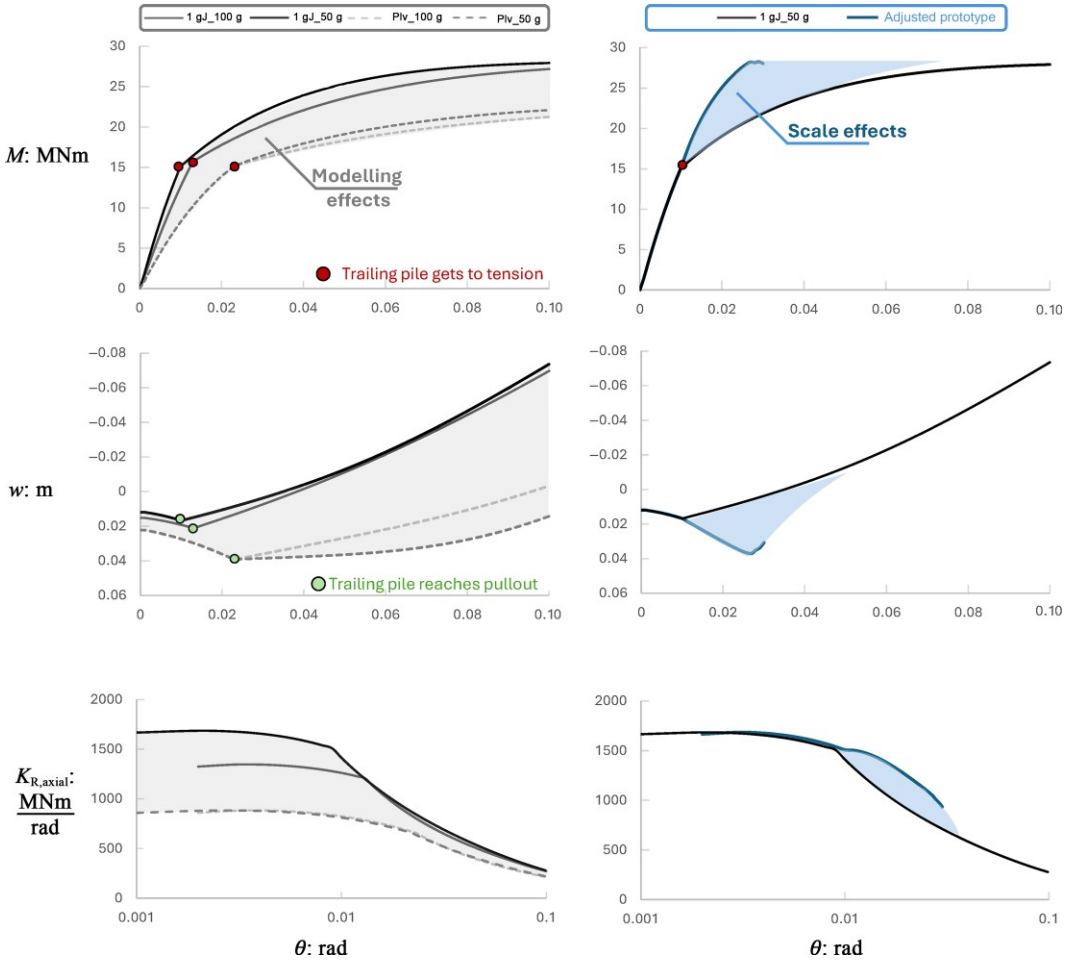

Figure 14. The effect of physical modelling choices and the unavoidable scale effects on the rocking response ($K_{R,\text{axial}}$) of an idealised 2 × 1 pile group, employing a simple analytical spring model assembly

required for the mobilisation of the shaft resistance, which is a function of the mean grain size.

Although centrifuge modelling is a powerful tool in deriving benchmark results and gaining insights into failure mechanisms, it is not completely immune to scale effects. Combining centrifuge modelling and numerical analyses, this paper has provided evidence of the role of such scale effects. The results are expected to increase awareness of the unavoidable limitations of centrifuge modelling, which may challenge its use for quantitative estimations, calling for careful transition from model to prototype scale.

Funding

The project presented in this paper was financially supported by the Swiss National Science Foundation (SNSF) under Grant No. 200021_188459. The authors would like to acknowledge the contribution of Markus Iten, Jürg Giger, Andreas Kieper, Ralf Herzog, and Dr. Simone Alber on the preparation and the successful execution of the centrifuge and interface tests presented in the paper.

References

ABAQUS (2019) *Standard User's Manual. Dassault Syst.* Simulia Corp., Providence, RI, USA

Agalianos A and Anastasopoulos I (2021) Numerical analysis of surface foundation subjected to strike–slip faulting: model boundaries, pre-softening volumetric response, parametric study. *Soil Dynamics and Earthquake Engineering* **151**: 106979.

Agalianos A, Korre E, Abdoun T and Anastasopoulos I (2023) Surface foundation subjected to strike–slip faulting on dense sand: centrifuge testing versus numerical analysis. *Géotechnique* **73(2)**: 165–182.

Alber S (2025) *Novel self-burrowing probe for in-situ soil investigation: Development and testing in a calibration chamber.* PhD Thesis, ETH Zurich, Zurich, Switzerland.

Augarde CE, Lee SJ and Loukidis D (2021) Numerical modelling of large deformation problems in geotechnical engineering: a state-of-the-art review. *Soils and Foundations* **61(6)**: 1718–1735.

Blanc M and Thorel L (2016) Effects of cyclic axial loading sequences on piles in sand. *Géotechnique Letters* **6(2)**: 163–167.

Bolton MD, Gui MW, Garnier J *et al.* (1999) Centrifuge cone penetration tests in sand. *Géotechnique* **49(4)**: 543–552.

Cesaro R, Di Laora R and Mandolini A (2025) Shaft resistance of bored piles in sand. *Acta Geotechnica*.

D'Arezzo FB, Haigh SK, Ishihara Y, Gaudin C and White D (2014) Modelling of jacked piles in centrifuge, In *8th International Conference on Physical Modelling in Geotechnics (ICPMG2014)*, Perth, Australia.

Del Giudice L, Wróbel R, Katsamakas AA, Leinenbach C and Vassiliou MF (2022) Physical modelling of reinforced concrete at a 1:40 scale using additively manufactured reinforcement cages. *Earthquake Engineering & Structural Dynamics* **51(3)**: 537–551, 10.1002/eqe.3578.

Di Laora R, de Sanctis L and Aversa S (2019) Bearing capacity of pile groups under vertical eccentric load. *Acta Geotechnica* **14(1)**: 193–205.

Di Laora R, Cesaro R, Iodice C, Iovino M and De Sanctis L (2025) A closed form solution for the generalised failure envelope of a pile group. *Soil Dynamics and Earthquake Engineering* **199**: 109623.

Drosos V, Chaloulos YK, Tasiopoulou P, *et al.* (2025) Analyses of spudcan penetration and its effect on an adjacent offshore WTG monopile foundation. *Proceedings of ISFOG 2025, Nantes, France*.

Fan S, Bienen B and Randolph MF (2021) Centrifuge study on effect of installation method on lateral response of monopiles in sand. *International Journal of Physical Modelling in Geotechnics* **21(1)**: 40–52.

Fioravante V (2002) On the shaft friction modelling of non-displacement piles in sand. *Soils and Foundations* **42(2)**: 23–33.

Garnier J and König D (1998) Scale effects in piles and nail loading tests in sand, *Proceedings International Conference Centrifuge 98*, Tokyo, T Kimura, O Kusakabe, J (eds), Balkema, Rotterdam, Vol. 1, pp. 205–210.

Garnier J, Gaudin C, Springman SM *et al.* (2007) Catalogue of scaling laws and similitude questions in geotechnical centrifuge modelling. *International Journal of Physical Modelling in Geotechnics* **7(3)**: 1–23.

Iovino M, Maiorano RMS, De Sanctis L and Aversa S (2021) Failure envelopes of pile groups under inclined and eccentric load. *Géotechnique Letters* **11(4)**: 247–253.

Klinkvort RT, Black JA, Bayton SM *et al.* (2018) A review of modelling effects in centrifuge monopile testing in sand. *Physical Modelling in Geotechnics* **1**: 720–723.

Klinkvort RT, Bienen B, Fan S *et al.* (2026) Centrifuge modelling considerations of laterally loaded monopiles in sand. *International Journal of Physical Modelling in Geotechnics* **26(2)**: 93–104.

Knappett JA, Reid C, Kinmond S and O'Reilly K (2011) Small-scale modeling of reinforced concrete structural elements for use in a geotechnical centrifuge. *Journal of Structural Engineering* **137(11)**: 1263–1271.

Lehane BM and White DJ (2005) Lateral stress changes and shaft friction for model displacement piles in sand. *Canadian Geotechnical Journal* **42(4)**: 1039–1052.

Lehane BM, Gaudin C and Schneider JA (2005) Scale effects on tension capacity for rough piles buried in dense sand. *Géotechnique* **55(10)**: 709–719.

Loli M, Knappett JA, Brown MJ, Anastasopoulos I and Gazetas G (2014) Centrifuge modeling of rocking-isolated inelastic RC bridge piers. *Earthquake Engineering & Structural Dynamics* **43(15)**: 2341–2359, 10.1002/eqe.2451.

Loukidis D and Salgado R (2008) Analysis of the shaft resistance of non-displacement piles in sand. *Géotechnique* **58(4)**: 283–296.

Madabhushi SPG, Houghton NE and Haigh SK (2006) A new automatic sand pourer for model preparation at University of Cambridge, *Proc. 6th International Conference on Physical Modelling in Geotechnics*, **1**: 217–222.

Qiu G, Henke S and Grabe J (2011) Application of a coupled Eulerian–Lagrangian approach on geomechanical problems involving large deformations. *Computers and Geotechnics* **38(1)**: 30–39.

Sakellariadis L, Bleiker E, Iten M *et al.* (2023) Testing pile foundations at the ETH Zurich drum centrifuge: recent developments. *International Journal of Physical Modelling in Geotechnics* **23(5)**: 219–247.

Sakellariadis L and Anastasopoulos I (2024a) Analytical 3D failure envelopes for RC pile groups under combined loading: a generalised design approach. *Soil Dynamics and Earthquake Engineering* **181**: 108570.

Sakellariadis L and Anastasopoulos I (2024b) On the mechanisms governing the response of pile groups under combined VHM loading. *Géotechnique* **74(9)**: 840–861.

Sakellariadis L, Gerolymos N and Anastasopoulos I (2026) Deformation analysis of RC piles and pile groups under combined loading: a nonlinear phenomenological modelling approach. *Soil Dynamics and Earthquake Engineering* **201**: 109875.

How can you contribute?

To discuss this paper, please email up to 500 words to the editor at support@emerald.com. Your contribution will be forwarded to the author(s) for a reply and, if considered appropriate by the editorial board, it will be published as discussion in a future issue of the journal.

International Journal of Physical Modelling in Geotechnics relies entirely on contributions from the civil engineering profession (and allied disciplines). Information about how to submit your paper online is available at www.emeraldgrouppublishing.com/journal/jphmg, where you will also find detailed author guidelines.